

# PSEUDOCHAOS

G M . Zaslavsky  
 M . Edelman

**ABSTRACT** A family of the billiard-type systems with zero Lyapunov exponent is considered as an example of dynamics which is between the regular one and chaotic mixing. This type of dynamics is called "pseudochaos". We demonstrate how the fractional kinetic equation can be introduced for the pseudochaos and how the main critical exponents of the fractional kinetics can be evaluated from the dynamics. Problems related to pseudochaos are discussed: Poincaré recurrences, continued fractions, log-periodicity, rhombic billiards, and others. Pseudochaotic dynamics and fractional kinetics can be applied to stream lines or magnetic field lines behavior.

## 1 Introduction

There are many examples that show transition to turbulence through the spatio-temporal chaos. The case of 2-dimensional Kolmogorov flow (P. Latt, Sirovich, and Fitzmaurice [1991]) displays a complicated alternation of different laminar and chaotic regimes following changes of a control parameter, which precede the dynamics known as the turbulent one. While the common opinion focuses on an exceptional role of coherent structures presented even in turbulent flows, the structures are still elusive and we still do not have a universal method for their depiction. Interesting ideas of the diagnostic of coherent structures can be found in recent publications (Sirovich [1989], Weiss, Provenzale, and Williams [1998], Haller [2000]). An indirect analysis of flows can be developed from the trajectories of passive particles (tracers). This approach is known also as the Lagrangian one versus the Eulerian one.

While the study of tracer dynamics is not sufficient to provide full information about the corresponding flow, it can reveal an important information about the flow transitions from one regime to another. An important example of the tracer dynamics appears for the so-called ABC (Arnold-Beltrami-Childress) flow (Arnold [1978]) for which the tracer dynamics coincides with stream line trajectories, is Hamiltonian (Zaslavsky, Sagdeev, Uspikov, and Chernikov [1991]), and consists of regular and chaotic domains in phase space for all nonzero values of the flow parameters (Zaslavsky, Sagdeev, Uspikov, and Chernikov [1991], Hénon [1966]). An area

of chaotic stream lines depends on the symmetry of flow, flow parameters, spectra, etc. (Agullo, Verga, and Zaslavsky [1997], Benkadda, Gabai, and Zaslavsky [1997], Benkadda and Beyer [2002], Zaslavsky, Sagdeev, Ustikov, and Cherenkov [1991]).

Similar to the tracer dynamics problem is the behavior of magnetic field lines for a given vector-field  $B(\mathbf{r})$  (Rosenbluth, Sagdeev, Taylor, and Zaslavsky [1966], Zaslavsky, Sagdeev, Ustikov, and Cherenkov [1991]) known to be chaotic long before the studies of chaos of Lagrangian particles. This analogy has been used to study a novel type of problem: randomness without sensitivity to the perturbation of initial conditions (Zaslavsky and Edelman [2001]). Field-lines of  $v$  or  $B$  can wind invariant surfaces of a topological genus more than one. In this case equations for the field lines are not integrable even if the Lyapunov exponent  $L = 0$  (Kozlov [1996]). We call trajectories to be pseudochaotic if  $L = 0$  but the equations that define the trajectories are not integrable.

It was shown for some cases of the pseudochaos (Zaslavsky and Edelman [2001]) that the ensemble of trajectories can be considered in a statistical manner and can be described by a kind of kinetic equation with fractional derivatives. Kinetics of trajectories reflects self-similarity of dynamics and superdiffusive equations for the moments of a distribution function along coordinates, i.e. superdiffusive transport. This article continues the work Zaslavsky and Edelman [2001] replacing the problem of the field-lines by a billiard type problem. There is no one-to-one correspondence between the field-line trajectories problem and the billiard one. Nevertheless, the study of particle dynamics in the billiard-type systems can provide a realistic insight on different possibilities of the dynamics as it has happened with the Sinai billiard.

We consider different billiard-type models with zero Lyapunov exponent. These models can be applied straightforwardly to such physical problems as ray dynamics in media with complex (fractal) boundary (Sapoval, Gobron, and Margolina [1991], Hebert, Sapoval, and Russ [1999]), light (Wilkinson, Fromhold, Taylor, and Micolich [2001a,b]) and sound (Zaslavsky and Abdullaev [1997]) propagation in nonuniform media, magnetic field lines in toroidal plasmas (Zaslavsky and Edelman [2001]), tracer dynamics in reconnected vortices (Zaslavsky and Edelman [2001]), etc. Similar problems proved to be interesting in problems of quantum chaos (Richters and Berry [1981], Wiersig [2000], Artuso, Guàmari, and Rebuzzini [2000], Artuso, Casati, and Guàmari [1997]) and general problems of anomalous transport (Artuso, Guàmari, and Rebuzzini [2000], Artuso, Casati, and Guàmari [1997], Zwanzig [1983], Zaslavsky and Edelman [2001]). There are also important works on the polygonal billiards (Gálerkin and Zemlyakov [1990], Katok [1980], Katok and Hasselblatt [1995], Gutkin [1996]) and related to it. The interval exchange transformation (IET) (Katok [1980], Zorich [1997]) which considers complexity, mixing, and transport.

In this paper we briefly review our previous results on the kinetics and

transport properties of the trajectories in a family of polygonal billiards and the corresponding Lorentz-type gases (Zaslavsky and Edelman [2001]), and present new results on the transport exponents and more complicated billiard-type models. It is worthwhile to mention here, that while there is a way of evaluating the transport exponents for IET (Zorich [1997]), these results cannot be applied immediately to the transport exponent of trajectories, and a special analysis of trajectories and their ensemble is necessary.

There are three separate problems related to the pseudochaotic kinetics, that will be briefly discussed here: transport in the rhombic billiard, log-periodic properties of continued fractions, and the origin of specific exponents for Poincaré recurrences.

## 2 FILAMENTED AND MERGED SURFACES, BILLIARDS, AND WEAK MIXING

We will speak about the particle dynamics having in mind a tracer or a field line as a particle trajectory. Examples of the filamented and merged surfaces are given in FIGURES 2.1 (a) and (b) correspondingly. The case (a) appears in the toroidal plasma confinement (Zaslavsky and Edelman [2001], Morozov and Soloviev [1966]) while the case (b) can appear in both plasma anduids. Under some conditions, the problem of the geodesics along surfaces can be reduced to the problem of trajectories in elastic billiards (Galperin and Zemlyakov [1990], Katok and Hasselblatt [1995]). Some examples of billiards are given in FIGURE 2.2 Billiards must have rational angles to be reducible to the equivalent dynamics along surfaces. Each of the billiards in FIGURE 2.2 can be periodically continued in two or one directions (FIGURES 2.3 and 2.4) creating a "generalized Lorentz gas" (GLG). As an example, let us point an evident connection between geodesics in FIGURE 2.1 (a), and trajectories in FIGURES 2.2 (a) and 2.3 (a).

Billiard trajectories can be studied by introducing a map of some interval into itself. For the case in FIGURE 2.2 (a) one can consider the map of the slit into itself, which belongs to the type of the interval exchange transformation: (IET) (Galperin and Zemlyakov [1990], Zorich [1997]). There are some common features between all four types of problems mentioned above: geodesics along complex surfaces, billiards, GLG, and IET. All of them correspond to the dynamics with zero Lyapunov exponent, i.e. two initially close trajectories diverge not faster than a power of time. All of them describe the so-called pseudo-integrable (but not integrable) situation (Katok [1980], Katok and Hasselblatt [1995]). All of them correspond to the dynamics with the weak mixing (Katok [1980], Katok and Hasselblatt [1995]) (more accurate formulation can be found in Gutkin [1996]).

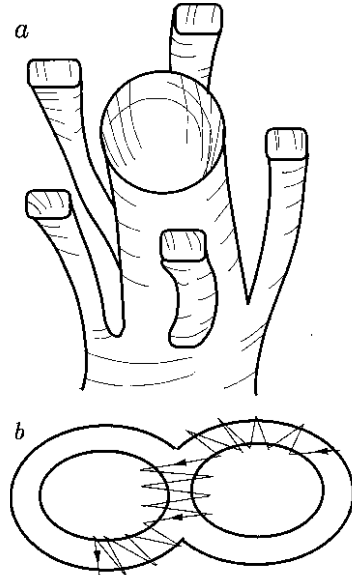


FIGURE 2.1. Examples of laminated (a) and merged (b) surfaces.

Let us recall (Comfeld, Fomin, and Sinai [1982]) that for almost arbitrary square integrable functions  $G_1(x)$  and  $G_2(x)$  of the coordinate  $x$  in phase space, the weak mixing means that

$$\lim_{n \rightarrow \infty} \frac{1}{n} \sum_{k=0}^{n-1} \langle \langle G_1(\hat{T}^k x) G_2(x) - \langle G_1 \rangle \langle G_2 \rangle \rangle \rangle^2 = 0 \quad (2.1)$$

while the mixing, or strong mixing, means

$$\lim_{n \rightarrow \infty} \langle \langle G_1(\hat{T}^n x) G_2(x) - \langle G_1 \rangle \langle G_2 \rangle \rangle \rangle = 0 \quad (2.2)$$

where  $\hat{T}$  is a time-shift operator and  $\langle \langle \cdot \rangle \rangle$  means the averaging over a corresponding measure. Weak mixing can be accompanied by arbitrary large and long-lasting bursts, i.e. fluctuations with large deviations from zero of the correlation function

$$R_n = \langle \langle \hat{T}^n x - \langle x \rangle \rangle \rangle^2 \quad (2.3)$$

These fluctuations exist simultaneously with the property that the average of  $R_n^2$  is zero. A sample of trajectory for the billiard in FIGURE 2.2(a) or GLG in FIGURE 2.3(a) is given in FIGURE 2.5 indicating arbitrary long-lasting almost periodic pieces of the trajectory.

There is no one-to-one correspondence between four different types of the above-mentioned systems: geodesics on a compact surface, billiard, GLG,

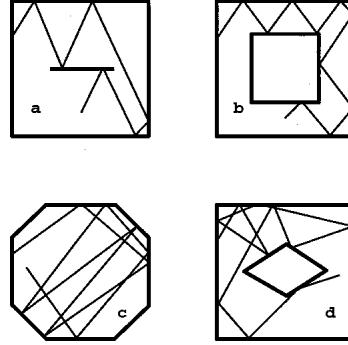


FIGURE 2.2. Examples of billiards of different types.

and IET. For example, properties of the IET obtained in [Zorich \[1997\]](#) are not sufficient to describe kinetics of trajectories in the corresponding billiard since the equation for the mapping time is not involved in IET. This explains a major difficulty in studying the billiards and GLG. Let us mention that IET dynamics and polygonal billiard dynamics is ergodic and weak mixing ([Katok \[1980\]](#), [Gutkin \[1996\]](#)), but there is only a conjecture that the complexity of the billiard trajectories is at most polynomial ([Gutkin \[1996\]](#), [Zaslavsky and Edelman \[2001\]](#)). Due to this, we will call pseudochaotic the dynamics of trajectories in billiards and GLG, when their Lyapunov exponent is zero and their complexity is, at most, algebraic. As it will be shown, such billiards can reveal fairly good statistical properties.

Let us provide a few examples for the billiard with a slit in [FIGURE 2.2\(a\)](#) and the corresponding GLG in [FIGURE 2.3\(a\)](#) [Zaslavsky and Edelman \[2001\]](#). Consider an element ' of the slit in [FIGURE 2.2\(a\)](#) and introduce a normalized distribution of the Poincaré recurrences to ' as

$$P_{\text{rec}}(t) = \lim_{\epsilon \rightarrow 0} \frac{1}{\epsilon} P_{\text{rec}}(\epsilon; t) \quad (2.4)$$

where  $P_{\text{rec}}(\epsilon; t)$  is a probability density to return a trajectory to the element ' does not matter from which side of '. Due to the above-mentioned conjecture, we can expect that

$$P_{\text{rec}}(t) = 1-t \quad ; \quad (t \neq 1) \quad (2.5)$$

with a recurrence exponent that satisfies the condition

$$2 < \quad (2.6)$$

due to the Kac lemma ([Comfeld, Fomin, and Sinai \[1982\]](#)):

$$\lim_{t \rightarrow \infty} \frac{1}{t} \int_0^t dt P_{\text{rec}}(t) < 1 \quad ; \quad (2.7)$$

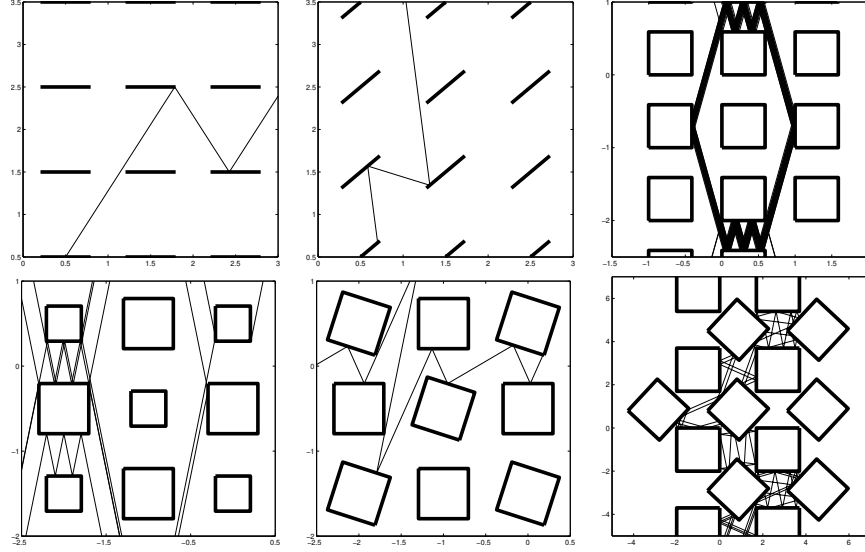


FIGURE 2.3. Periodically continued billiards form a "generalized Lorentz gas" (GLG).

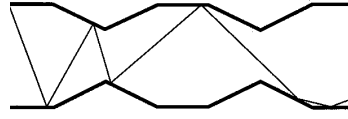


FIGURE 2.4. Ray propagation billiard model with a piecewise periodic nonuniformity.

ie. the mean recurrence time is finite for the bounded area preserving dynamics.

To study transport properties in billiards, consider a bundle of trajectories, launched with initially close angles, as an ensemble [Zaslavsky and Edelman 2001]). For the same case in FIGURE 2.3(a) we can consider moments  $h^{2m}$  with an integer  $m$ . It was shown in Zaslavsky and Edelman [2001] that

$$h^{2m} \propto t^{(m)} \quad (2.8)$$

with

$$(m) = m(1); \quad (1) = 1:7; \quad 2:7; \quad (2.9)$$

and with the connection

$$(1) + 1 \quad (2.10)$$

Similar value of  $(1)$  was obtained in Artuso, Guàmari, and Rebuzzini [2000]. Some deviations of  $(m)$  from the linear law (2.9) will not be dis-

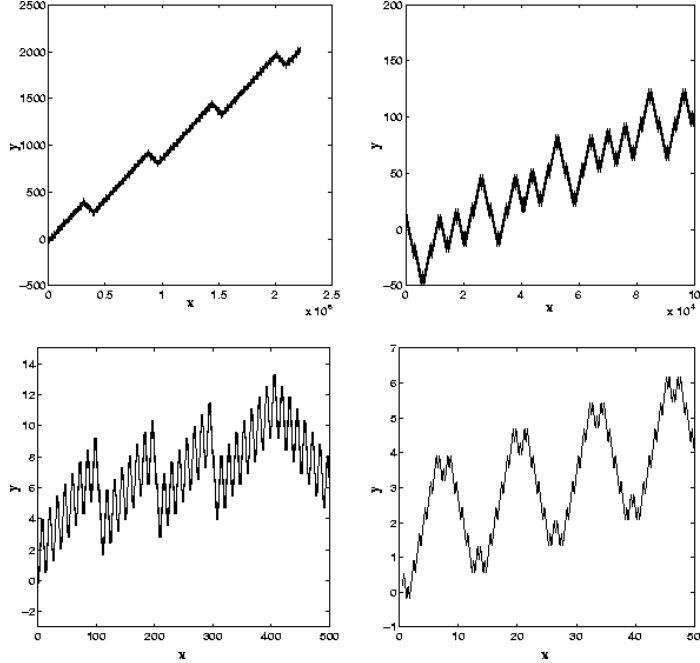


FIGURE 2.5. Samples of a trajectory with different space (time) scales for the billiard in FIGURE 2.2 (a).

cussed here (see more in [Zaslavsky and Edelman \[2001\]](#)). The values (2.10) are almost independent on the length of the slit and the launching angle. This universality will be commented later as well as deviations from (2.8)–(2.10). The results (2.8)–(2.10) can be immediately transferred to the billiards in FIGURE 2.2 (b) and to the GLG in FIGURES 3 (b) and 3 (c), since trajectories do not change initial tangent of the angles during the scattering. Formula (2.8) shows anomalous transport ( $1 \notin 1$ ) of the superdiffusion type and an approximate self-similarity since  $(m) \sim (1)$ . All these properties and deviations from them will be discussed in the forthcoming sections.

### 3 MORE BILLIARDS

In this section we would like to present more different types of billiards and their statistical properties. These results can be considered as a kind of "experimental material".

Let us start from the two equal-squares-lattices in FIGURES 3 (e,f) with infinite and finite horizons, respectively. Some squares are rotated by an angle of irrational tangent with respect to the others. Due to that, almost

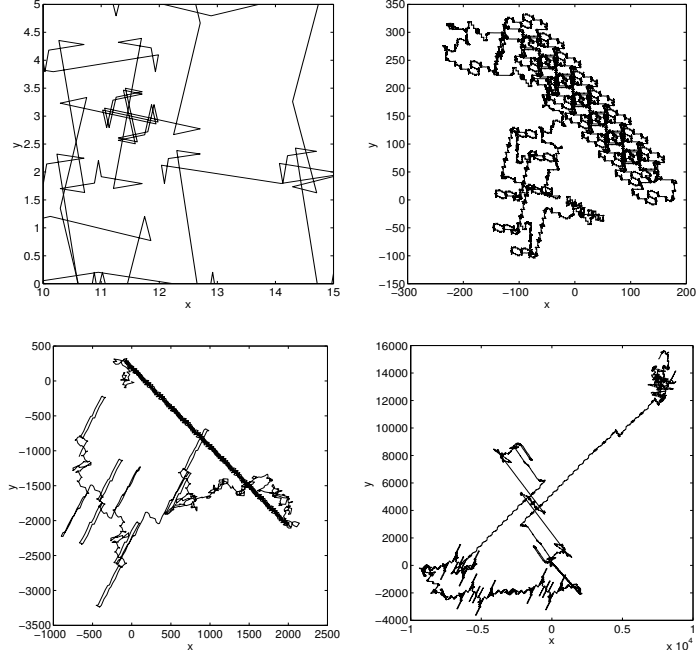


FIGURE 3.1. A trajectory for the billiard in FIGURE 2.3(e) with an infinite horizon. Its different zooms show flights that last about  $10^4$ .

all trajectories rotate ergodically in the coordinate space in contrary to the billiards in FIGURES 3 (a-d). Samples of trajectories are given in FIGURES 3.1, 3.2. There are two important features common for both figures. First, the trajectories have arbitrary long flights. We call 'a flight' any long part of the trajectory that, after small scale averaging, is almost regular. Such pieces of trajectories correspond to an intermittent dynamics and they are responsible for the distribution functions with tails and for fractional kinetics [Zaslavsky [1994a,b], Saichev and Zaslavsky [1997]]. The trajectories have similarity in small and in large time and space scales. The self-similarity is less evident in FIGURES 3.1, 3.2 than in FIGURE 2.5. More delicate description of the trajectories can be obtained from simulations.

In FIGURE 3.2 we present two types of statistical properties of trajectories for the infinite horizon billiard. The moments of the coordinate displacements

$$h x^{2m} i \quad t^{x(m)} ; \quad h y^{2m} i \quad t^{y(m)} \quad (3.1)$$

with

$$x(m) = y(m) \quad m \quad (1) \quad (3.2)$$

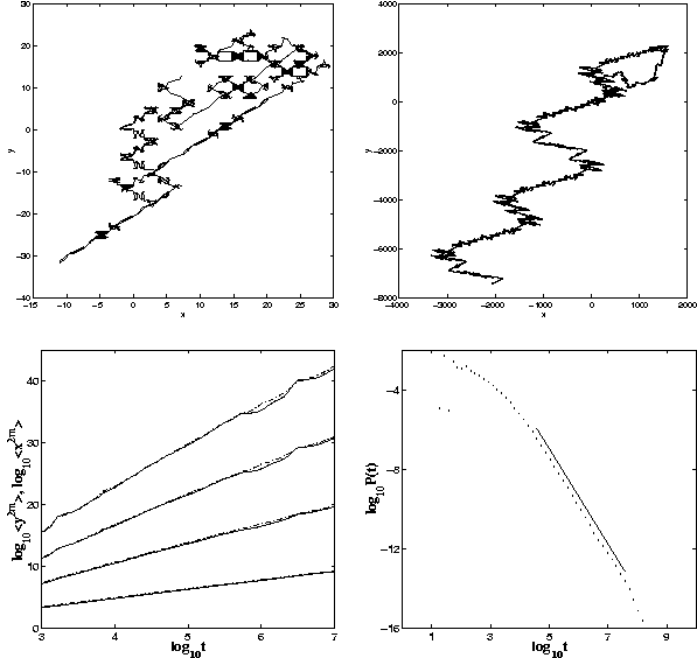


FIGURE 3.2. A trajectory with two, small and large, time intervals (two top plates), and the moments  $h_x^{2m}$  (regular lines),  $h_y^{2m}$  (dash-point lines), and distribution of the recurrences  $P(t)$ . The data for the two bottom plates are obtained after averaging over 8,192 trajectories and time  $3.4 \cdot 10^8$  for each. Four curves of the moments vs. time correspond to  $m = 1; 2; 3; 4$  from the bottom.

and

$$(1) \quad 1.5 : \quad (3.3)$$

Considering one cell of the lattice (similar to the billiards in FIGURE 2.1), one can obtain a distribution function of Poincaré recurrences (see (2.5)). The simulation gives

$$2.4 \quad (3.4)$$

in a good agreement with the relation (2.10). Similar to (3.3), values of (1) 1.5 were obtained for the billiard with the infinite horizon (FIGURE 2.3(e)) with the recurrence exponent 2.5.

#### 4 CONTINUED FRACTION S AND SCALINGS

It is convenient to consider first a theory for the billiard with a slit in FIGURES 2.2(a) or 2.3(a) since the kinetics in the billiard is one-dimensional

along  $y$  and velocity  $v_x$  along  $x$  is constant. This billiard attracts the attention fairly long ago (see Zwanzig [1983] and following publications Hanany and McCraw [1990], Richters and Berry [1981], Wiersig [2000], Artuso, Guameri, and Rebuzzini [2000], Artuso, Casati, and Guameri [1997]). In our work Zaslavsky and Edelman [2001] we use the properties of the continued fractions (Khinchin [1964], Levy [1937]) to obtain the recurrence distribution and kinetic properties of the trajectories. In this section we will repeat and extend the results of Zaslavsky and Edelman [2001].

Let us recall the samples of the trajectory in FIGURE 2.5. Trajectories with an angle  $\#$  to  $x$  will be called rational/irrational if  $\tan \#$  is rational/irrational. We will consider only irrational ensembles, i.e. bunches of trajectories with irrational  $\tan \#_j$  and  $\#_j \in (\#-2, \#+2)$  within an interval  $\#$ .

Let

$$\tan \# = a_0 + \dots ; \quad (4.1)$$

where  $a_0$  is the integer part of  $\tan \#$ , and  $\# \in (0;1)$  can be written as a continued fraction

$$= 1 = (a_1 + 1 = a_2 + \dots) = [a_1; a_2; \dots] \quad (4.2)$$

For irrational the sequence  $[a_1; a_2; \dots]$  is infinite and its infinite approximation is

$$_n [a_1; \dots; a_n] = p_n/q_n \quad (4.3)$$

with mutually simple  $p_n/q_n$ . In the following, we use three important results on continued fractions (Levy [1937]):

(a) Estimate for the accuracy of the  $n$ -th convergent

$$j \quad p_n/q_n \quad 1 = q_n q_{n+1} ; \quad (4.4)$$

(b) A symptotic property of the sequence  $f a_j g$

$$\lim_{n \rightarrow \infty} (a_1 \dots a_n)^{1/n} = \sqrt[n]{1 + \frac{1}{k^2 + 2k}} = 2.63 \dots \quad (4.5)$$

(c) A symptotic property of the sequence  $f q_j g$

$$\lim_{n \rightarrow \infty} \frac{1}{n} \ln q_n = \sqrt{2 \ln 2} = 1.186 \dots \quad (4.6)$$

Formulas (4.5) and (4.6) indicate a remarkable scaling structure of continued fractions

$$\begin{aligned} a_1 \dots a_n & \quad \frac{n}{a} q_a(n) \\ q_n & \quad \frac{n}{q} q_q(n) \end{aligned} \quad (4.7)$$

with scaling parameters  $a$ ;  $q$  and some subexponential functions  $g_a(n); g_q(n)$ .

For an arbitrary irrational trajectory with an angle  $\#$ , consider its  $n$ -th approximate  $\#_n$  and a corresponding rational trajectory with an angle  $\#^{(n)}$  such that  $\tan \#^{(n)} = a_0 + \#_n$ . This trajectory is periodic with the period Galperin and Zemlyakov [1990]

$$T_n = \text{const} \quad (4.8)$$

with the  $\text{const} = 2$  or  $4$ , depending on how the upper and the lower sides of the slit will be considered. The approximate trajectory is close to the original one for a time much larger than  $T_n$  due to the fast convergence (4.4). That is just the property that one can see from the samples in FIGURE 2.5. The property (4.8) was used in Zaslavsky and Edelman [2001] to get the scaling for different quasi-periods of any irrational trajectory

$$T_n = \frac{n}{T} g_T(n) \quad (4.9)$$

which is similar to (4.7) with the time-scaling parameter  $T$

$$\ln T = \ln q = \frac{2}{T} = 12 \ln 2 = 1.186 \dots \quad (4.10)$$

Simulation for  $\# = 4.153087 \dots$  gives  $\ln T = 1.17 \quad 0.08$  in an excellent agreement with (4.6).

Expression (4.10) defines hierarchical structures of different lengths in time. Corresponding hierarchical structures should exist for the lengths  $\lambda_n$  of the flights along  $y$ . Nevertheless, there exist an ambiguity of the flight lengths  $\lambda_n$  since trajectories can have strong coordinate oscillations for the same time duration of flights. To find a corresponding scaling parameter  $y$ , we assume that

$$\ln y = \overline{\ln \text{den}} \quad (4.11)$$

where  $\text{den}$  means scaling parameter of different possible denominators of the rational convergent of  $\#$ , obtained at the same hierarchical level along a trajectory, and the bar means averaging over such possibilities. For example, at the hierarchical level  $n$ ,  $\lambda_n$  has  $q_n$  as the minimal denominator and  $a_1 \dots a_n$  as the maximal denominator since

$$a_1 \dots a_n \quad q_n : \quad (4.12)$$

Applying (4.7) we obtain

$$\ln \text{den} = \ln T ; \quad \max \text{den} = a \quad (4.13)$$

The simplest estimate is

$$\ln y = \overline{\ln \text{den}} = \frac{1}{2} (\ln T + \ln a) = 1.07 \dots \quad (4.14)$$

The obtained information can be applied to construct the kinetic evolution of an ensemble of trajectories.

All the numbers (4.10), (4.14) should be the same for the billiards with a slit (FIGURES 2.2(a), 2.3(a)) and with equal squares (FIGURES 2.2(b), 2.3(c)).

## 5 F R A C T I O N A L K I N E T I C S I N B I L L I A R D S

The fractional space-time kinetic equation was introduced in Zaslavsky [1992] and detailed for dynamical systems in Zaslavsky [1994a,b], Saichev and Zaslavsky [1997] in order to describe self-similar non-Gaussian processes with strong intermittency. For a billiard of the type in FIGURES 2.2(a,b) and 2.3(a-c), the equation has the form

$$\frac{\partial f(y;t)}{\partial t} = D \frac{\partial f(y;t)}{\partial y^j} \quad (5.1)$$

where  $f(y;t)$  is a distribution function, and fractional derivatives can be considered using their Fourier transform (F.T.):

$$F \cdot T : \frac{\partial}{\partial t} = i! ; \quad F \cdot T : \frac{\partial}{\partial y^j} = ijkj \quad (5.2)$$

Usually, we are interested in asymptotics  $t \rightarrow 1$ ,  $y \rightarrow 1$ . Since the moments

$$h_{ij}^{2m} i = \int y^{2m} f(y;t) dy \quad (5.3)$$

diverge for  $2m > 1$  (Zaslavsky [1994a,b], Saichev and Zaslavsky [1997]), it is convenient to consider truncated distribution  $f(y;t)$ , ( $y < y_{\max}$ ) and moments with  $m_{\min}$  and  $m_{\max} > 2$ , all of which are finite and present a self-similar evolution (see for example FIGURE 3.2 which shows  $m = 1, 2, 3, 4$ ). With this comment we can get from (5.1)

$$h_{ij}^{2m} i = \text{const} \cdot t \quad (5.4)$$

and expect that

$$h_{ij}^{2m} i = t^{(m)} \quad (5.5)$$

with

$$(m) = m - 1 \quad (5.6)$$

(compare to (3.2)).

In fact, the situation is more complicated (Zaslavsky and Edelean [2000]). The self-similarity of  $f(y;t)$  means that Eq. (5.1) is invariant under the transformation

$$t' = \tau t ; \quad y' = \gamma y \quad (5.7)$$

with appropriate values of the scaling parameters  $\tau$ ;  $\gamma$ . Then from (5.1), (5.7) we obtain the  $x$ -point condition

$$\lim_{n \rightarrow 1} (y = \tau)^n = 1 \quad (5.8)$$

or

$$\ln_T = \ln_y + 2ik \quad (5.9)$$

with an integer  $k$ . Then the solution for (5.1) can be written in the form (Zaslavsky and Edelman [2001], Zaslavsky and Edelman [2000])

$$h_{ij}^x = \sum_{k=1}^{\infty} C_k t^k \quad (5.10)$$

$$k = (1) = 2 + 2ik = \ln_T$$

with

$$= 2 \ln_y = \ln_T ; \quad (5.11)$$

and some expansion coefficients  $C_k$ . The expression (5.10) can be transformed into

$$h_{ij}^x = t \sum_{k=0}^{\infty} D_k \cos 2k \frac{\ln t}{\ln_T} + \phi_k \quad (5.12)$$

with new coefficients  $D_k$  and phases  $\phi_k$ . The last expression shows the so-called log-periodicity with a period

$$T_{\log} = \ln_T \quad (5.13)$$

and with corresponding terms  $D_{k \neq 0}$  that typically are small. For the self-similar behavior of the moments of  $f(y; t)$  we also expect

$$h_{ij}^{2m} = t^{(m)} \sum_{k=0}^{\infty} D_k \cos 2k \frac{\ln t}{\ln_T} + \phi_k \quad (5.14)$$

with coefficients  $D_k$  and phases  $\phi_k$ , and

$$(m) \quad m(1) = m = 2 \ln_y = \ln_T : \quad (5.15)$$

Expressions (5.13), (5.14) are just the ones that should be tested by simulations. As it was mentioned in the previous section, the results should be the same for the billiards in FIGURES 2.2(a) (2.3(a)) and 2.2(b) (2.3(c)). The results of simulations are presented in FIGURE 5.1. In FIGURE 5.1(a) we observe power law decay of the distribution of Poincaré recurrences with  $2:7$ . There are also some oscillations which make deviations from this value of  $2:7$ . FIGURE 5.1(b) shows moments for  $m = 1; 2; 3; 4$  and the self-similarity with  $m = (1) = 1:7$ . There are small deviations from the linear dependence of  $(m)$  on  $m$  for  $m = 2; 3$  and  $4$ ,  $(2) = 3:5$ ;  $(3) = 5:5$ ;  $(4) = 7:4$ .

Let us consider the formula (5.15) and use for  $T$  and  $y$  the values predicted by the continued fraction theory (4.10) and (4.14). It gives  $m =$

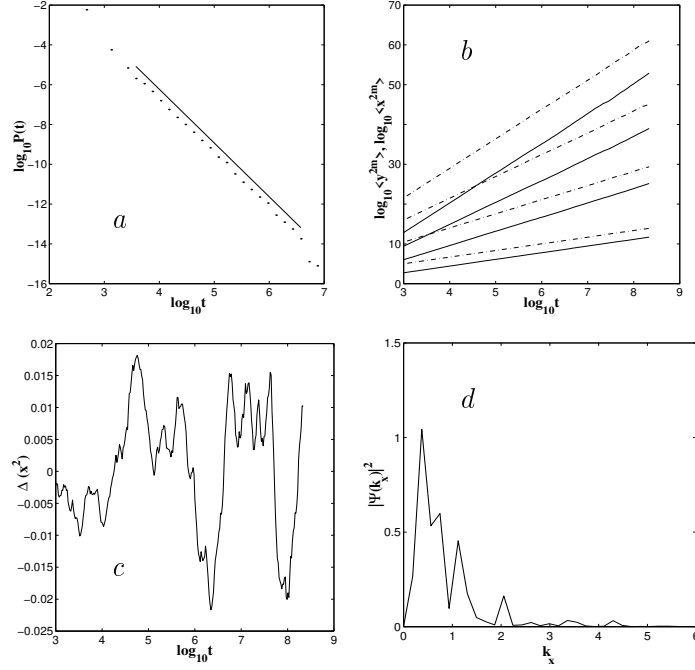


FIGURE 5.1. Statistical properties of the square billiards: (a) density distribution function of the recurrences  $P(t)$ ; (b) moments of  $x$  (full lines) and  $y$  (point-dash lines) for  $m = 1; 2; 3; 4$  starting from the bottom; (c) fluctuations of the second moment of  $x$  vs. time; and (d) their Fourier spectrum. The data are obtained for 4,048 trajectories during the time  $10^8$  for each.

(1) = 1.8 which is in a good agreement with the results of simulation in FIGURE 5.1 (b). The values of

$$2.7; \quad 1.7 \quad (5.16)$$

are also in agreement with (2.10). It is more delicate issue to evaluate the log-periodicity. There are small oscillations in the second moments  $\langle x^2 \rangle, \langle y^2 \rangle$  in time dependence. In FIGURE 5.1 (c) we show their amplitude

$$\langle x^2 \rangle = \hbar x^2 i \text{ const} : \quad (5.17)$$

These oscillations do not look absolutely random due to the presence of structures. To find it, consider the Fourier transform of (5.17), i.e.

$$\langle k_x \rangle = \int dt e^{i k_x \log_{10} t} \langle x^2 \rangle \quad (5.18)$$

FIGURE 5.1 (d) shows the almost continuous spectrum with some regular peaks. The characteristic width of the regular part of the spectrum is

$k_x = 2$ . From (5.13) and (4.10), the width of the spectrum in the decimal logarithm basis should be  $1 = \log_{10} T = 2$  in the excellent agreement with the data of simulations. Similar agreement was obtained in [Zaslavsky and Edelman 2001] for the billiard of FIGURE 2.2(a) (2.3(a)) type.

## 6 RHOMBIC BILLIARD

This type of billiard is shown in FIGURE 2.2(c,d). Its one-dimensional periodic continuation (FIGURE 2.4) can be interesting for different applications such as wave/ray propagation in nonuniform media. Two-dimensional periodic rhombic scatterers with an external field and small values of the Lyapunov exponents were considered in [Lepri, Rondoni, and Benettin 2000].

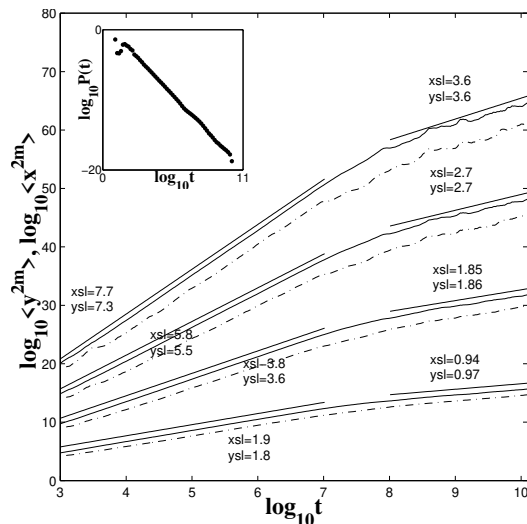


FIGURE 6.1. Moments and distribution density  $P(t)$  of the recurrences for the rhombic billiard. The data are obtained from 512 trajectories during the time  $10^{10}$  for each.

The most interesting case is the irrational billiard, i.e. the case with an irrational ratio of the rhombic diagonals. The rhombic billiard should inherit properties of the triangular billiards considered in [Artuso, Guameri, and Rebuzzini 2000], [Artuso, Casati, and Guameri 1997], [Casati and Rosen 1999]. In FIGURE 6.1 we presented the recurrences distribution  $P(t)$  for which the slope recurrence exponent is  $= 2 - 0.1$ , and the coordinates moments  $\langle x^{2m} \rangle, \langle y^{2m} \rangle$  versus time. The latter shows two exponents: during the time interval  $0 < t < 10^7$ ,  $(1) = 1.8 - 1.9$ , and after that time  $10^7 < t < 10^{10}$ ,  $(1) = 0.95 - 0.05$ . We cannot guarantee that this exponent

is not an intermediate one, but it satisfies the condition (2.10) and both values of  $\alpha$  and  $\beta$  for large  $t$  are close to the values obtained in Casati and Rosen [1999] for the triangular billiard. These values will be discussed in Section 8.

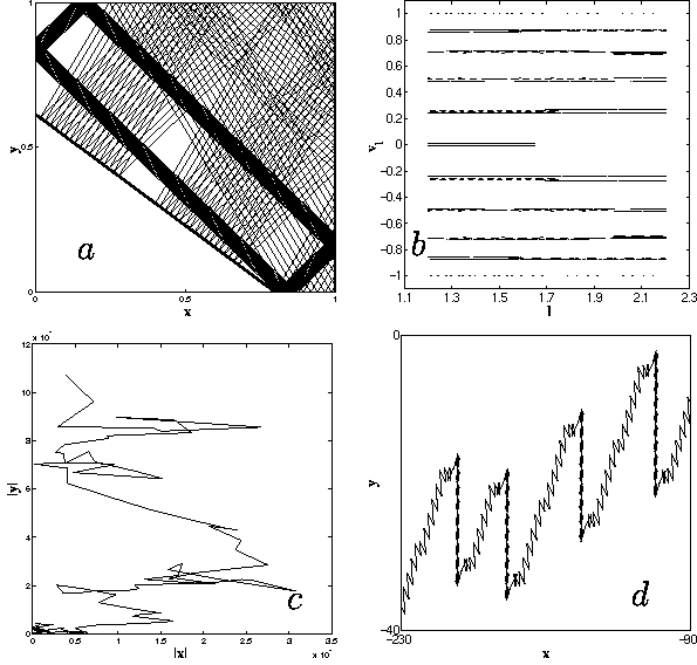


FIGURE 6.2. Rhombic billiard with the  $x$ -diagonal  $= 1.6$  and  $y$ -diagonal  $= 1.2290472$  (a) a sample trajectory in a square shows slow evolution; (b) phase plane  $v$ ,  $x$  (' is the upper side of the square in (a)) shows slow evolution in the angle (i.e. along  $v$ ); (c) a sample trajectory in large scale; and (d) its zoom .

In FIGURE 6.2 we present samples of trajectories which show trappings and very slow escape from the trapping domains. This feature of the trajectories can be especially well observed from FIGURE 6.2(b) of the Poincaré section: each point corresponds to a trajectory crossing of the interval ' $x$ ':  $y = 1$ ,  $x \in (0;1)$  in FIGURE 6.2(a). There is extremely slow process of fix ing along the velocity  $v$  and the filling of the phase space is performed mainly along  $x$  for some special values of  $v$ . We will speculate on the recurrences estimate in Section 8, applying for this type of dynamics.

## 7 BACK TO THE CONTINUED FRACTALS

Here we present a comment to the continued fractions properties. Since trajectories in the billiard with a slit or a square bear scaling properties of the continued fractions from one side, and the log-periodicity from another side, one can expect that the statistical features of continued fractions should have similar type of the log-periodic oscillations.

Consider a large number (ensemble) of irrational numbers  $f^{(1)} < 1g$ . For each representative  $^{(1)}$  of the ensemble, consider their  $n$ -th approximate, i.e.

$$^{(1)} = [a_1^{(1)}; a_2^{(1)}; \dots; a_n^{(1)}] = p_n^{(1)} = q_n^{(1)} : \quad (7.1)$$

The new ensemble is the ensemble of the denominators  $q_n^{(1)}g$ . We can introduce a distribution function  $(q; n)$ , i.e. a probability density to have value  $q$  for the denominator of the convergent of irrational numbers at  $n$ -th step. The variable  $n$  plays a role of the discrete time.  $(q; n)$  should be a universal function for which we can introduce moments

$$\ln \frac{2^m}{q} i = \int_0^1 q^{2^m} (q; n) dq \quad (7.2)$$

The asymptotic property (4.7) suggests that

$$\ln \frac{2^m}{q} i = nc(1 + d_n) \quad (7.3)$$

with

$$c = \ln q \quad (7.4)$$

and  $d_n$  depends slowly on  $n$ . The conjecture is that the Fourier spectrum of  $d_n$  consists of two parts: quasi-periodic and continuous, similar to what we have for the billiards.

To verify the conjecture, we considered  $10^3$  different irrational numbers  $f^{(1)} < 1$  ( $= 1; \dots; 10^3$ ) and their approximates with the quadrupole precision. The behavior of moments  $\ln \frac{2^m}{q} i$  is presented in FIGURE 7.1 up to  $n = 150$ . The plot shows oscillations which are stronger for higher moments. The slope corresponds to the value (7.4) with an accuracy up to the level of oscillations. The value of oscillations with respect to the straight line is shown in FIGURE 7.1(a), and their Fourier transform is in FIGURE 7.1(b). The figures show a finite, quickly decaying peaks of modulation of the continuous type spectrum. The last one has been proved in [Ibragimov and Linnik \[1971\]](#).

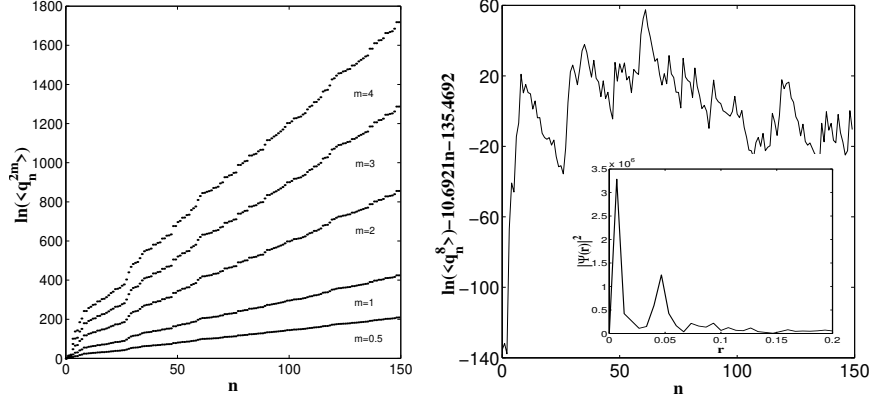


FIGURE 7.1. Statistical features of the continued fractions: moments of the denominators  $q_n^{2m}$  vs. number  $n$  of the approximation level and fluctuations of the 8-th moment with the spectral function.

## 8 ESTIMATES FOR THE DISTRIBUTION OF RECURRENCES

In this section we provide rough estimates for the distribution of recurrences  $P(t)$  or, more accurately, for possible values of the recurrence exponent when the  $P(t)$  behaves algebraically. As it was mentioned in (2.6) the value of  $\beta$  should exceed 2 for the bounded Hamiltonian dynamics.

A qualitative way to obtain  $P(t)$  is to consider an enveloped phase volume  $\Omega(t)$  evolution with time and a probability of a particle to return back from this volume to the initial one  $\Omega_0 < \Omega(t)$ . One can consider a small ball of the size  $\epsilon$  that moves in phase space and cover it with time. There are different possibilities:

$$\begin{aligned} \Omega_1(t) &= \text{const: } t^{1-\beta} \\ \Omega_2(t) &= \text{const: } t^{2-\beta} \\ \Omega_3(t) &= \text{const: } t^{3-\beta} \\ \Omega_4(t) &= \text{const: } t^{4-\beta} \end{aligned} \quad (8.1)$$

where  $\beta$  are considered as corrections to four different main values. The case of  $\Omega_1(t)$  corresponds to almost one-dimensional coarse-grained dynamics. It seems that this case happens in the rhombic and triangular billiards and FIGURES 6.2 (b,c) confirm this statement. The same case can appear also in one-dimensional dynamics (see Young [1999] and some rigorous results therein).

The case of  $\Omega_2(t)$  corresponds to the linear evolution along one coordinate and the diffusional type evolution along the other coordinate along which the phase volume growth is proportional to  $t^{1-\beta}$ . This is one of the

most typical case for many systems with intermittent chaotic dynamics [Zaslavsky and Edelman 2000]). The third case of  $\beta_3(t)$  corresponds to the almost linear phase space coverage along one coordinate and then the similar coverage along another coordinate. The alternations of the coordinates can be randomly distributed but the result provides almost  $t^2$ -growth of  $\beta_3(t)$ . It seems that it is the case of the original Sinai billiard when  $\beta_3 = 0$  [Chernov and Young 2000]). The case of  $\beta_4(t)$  can appear in special situations of 1 1/2 degrees of freedom or in higher dimension system [Rakhlin 2001]).

For (8.1) we obtain the return probability during the time interval  $(0; t)$  as  $\phi = \beta_j(t)$  and finally

$$P(t) = \frac{d}{dt} \frac{\phi}{\beta_j(t)} \quad \text{const} = t^j \quad (8.2)$$

with the corresponding values of  $j$

$$\begin{array}{rcc} & 8 & \\ & \gtrless & \\ j & \begin{array}{c} 2+1 \\ 5=2 \quad 2 \\ \gtrless 3 \quad 3 \\ \vdots \quad 4 \end{array} & \end{array} \quad (8.3)$$

where  $j$  represents the corrections to the main exponents. We have to recall that for some cases exact values of the exponents have no meaning since the log-periodic oscillations of the distributions  $P(t)$ .

## 9 CONCLUSIONS

The randomness with zero Lyapunov exponent, that we call pseudochaos, can appear in numerous applications. Its analysis provides a link between the structure of stream lines of flows, magnetic field lines, billiards, continued fractions, and fractional kinetics. It seems that the dynamical processes that can be described by the fractional type kinetic equation reveal a polynomial complexity, while the chaotic hyperbolic dynamics has the exponential growth of the coarse-grained phase volume.

Acknowledgments: We appreciate V. A. Fraiman and L.-S. Young for numerous and useful discussions, B. Sapoval and J. Wiersig for correspondence and information about their publications.

This work was supported by the U.S. Navy Grants No. N00014-96-1-0055, N00014-97-1-0426, and the U.S. Department of Energy Grant No. DE-FG02-92ER54184. The simulation was supported in part by the National Science Foundation (NSF) cooperative agreement No. ACI-9619020

through computing resources provided by the National Partnership for Advanced Computational Infrastructure at the San Diego Supercomputer Center, and by NERSC .

## References

Agullo, O., A. D. Verga, and G. M. Zaslavsky [1997], Chaotic advection and transport in helical Beltrami flows: A Hamiltonian system with anomalous diffusion, *Phys. Rev. E* 55, 5587-5596.

Arnold, V. I. [1978] Mathematical Methods in Classical Mechanics. Springer, New York.

Artuso, R., J. Cacaci, and I. Guarneri [1997], Numerical study on ergodic properties of triangular billiards, *Phys. Rev. E* 55, 6384-6390.

Artuso, R., I. Guarneri, and L. Rebuzzini [2000], Spectral properties and anomalous transport in a polygonal billiard, *Chaos* 10, 189-194.

Benkadda, S. and P. Beyer [2002], *Chaos*, to appear.

Benkadda, S. S., P. Gabbai, and G. M. Zaslavsky [1997], Passive particle dynamics in a flow exhibiting transition to turbulence, *Phys. Plasma* 4, 2864-2870.

Casati G., and T. P. Rosen [1999], Mixing property of triangular billiards, *Phys. Rev. Lett.* 83, 4729-4732.

Chernov N. and L.-S. [2000], Decay of correlations in Lorentz gases and hard balls, preprint, 32 pages.

Comfeld, I. P., S. V. Fomin, and Ya. G. Sinai [1982], Ergodic Theory. Springer, New York.

Galperin, G. A. and A. N. Zemlyakov [1990]. Mathematical Billiards. Nauka, Moscow (in Russian).

Gutkin, E. [1986], Billiards in polygons, *Physica D* 19, 311-333.

Gutkin, E. [1996], Billiards in polygons: Survey of recent results, *J. Stat. Phys.* 83, 7-26.

Haller, G. [2000], Finding finite-time invariant manifolds in two-dimensional velocity fields, *Chaos* 10, 99-108.

Haennay, J. H. and R. J. M. CC raw [1990], Barrier billiards - a simple pseudo-integrable system, *J. Phys. A* 23, 887-899.

Hebert, B ., B . Sapoval, and S. Russ [1999], Experimental study of a fractal acoustical cavity, *J. Acoust. Soc. Am.* 105, 1567{1574.

H enon, M . [1966], Sur la topologie des lighes de courant dans un cas particulier, *Compt. Rend. Acad. Sci. A Math.*, 262, 312{314.

Ibragimov, I. H . and Yu. V . Linnik [1971], *Independent and Stationary Sequences of Variables*. Wolters-Noordho Publ., Groningen.

K atok, A . [1980], Interval exchange transformations and some special flows are not mixing, *Isr. J. Math.* 35, 301{310.

K atok, A . [1987], The growth rate for the number of singular and periodic orbits for a polygonal billiard, *Commun. Math. Phys.* 111, 151{160.

K atok, A . and B . Hasselblatt [1995], *Introduction to the Modern Theory of Dynamical Systems*. Cambridge Univ. Press, Cambridge.

K hindin, A . Ya. [1964], *Continued Fractions*. University of Chicago Press, Chicago.

K ozlov, V . V . [1996], *Symmetries, Topology, and Resonances in Hamiltonian Mechanics*. Springer, Berlin.

Lepri, S ., L. Rondoni, and G . Benettin [2000], The Gallavotti-Cohen fluctuation theorem for a nonchaotic model, *J. Stat. Phys.* 99, 857{872.

Levy, P . [1937], *Theorie de l'Addition des Variables Aleatoires*. Gauthier-Villiers, Paris.

M orozov, A . I. and L. S. Soloviev [1966], The structure of magnetic fields, in *Reviews of Plasma Physics*, ed. M A . Leontovich. Consultants Bureau, New York, vol 2, p. 1{101.

P latt, N ., L. Sirovich, and N . F itzmaurice [1991], An investigation of chaotic Kolmogorov flows, *Phys. Fluids A* 3, 681{696.

R akhlin, D . [2001]. Enhanced diffusion in smoothly modulated superlattices *Phys. Rev. E* 63, 011112.

R ichens, P . J. and M . V . Berry [1981], Pseudo-integrable systems in classical and quantum mechanics, *Physica D* 2, 495{512.

Rosenbluth M ., R . Z . Sagdeev, J. B . Taylor, and G . M . Zaslavsky [1966], Destruction of magnetic surfaces by magnetic field irregularities, *Nucl. Fusion* 6, 297{300.

Saichev, A . I. and G . M . Zaslavsky [1997], Fractional kinetic equations: solutions and applications, *Chaos* 7, 753{764.

Sapoval B., Th. Gobron, and A. M. Argolina [1991], Vibrations of fractal drums, *Phys. Rev. Lett.* 67, 2974{2977.

Sirovich, L. [1989], Chaotic dynamics of coherent structures, *Physica D* 37, 126{145.

Weiss, J. B., A. P. Rovenzale, and J. C. M. de William [1998], Lagrangian dynamics in high-dimensional point-vortex systems, *Phys. Fluids* 10, 1929{1941.

Wiersig J., [2000], Singular continuous spectra in a pseudo-integrable billiard, *Phys. Rev. E* 62, R21{R24.

Wilkinson, P. B., T. M. Fromhold, R. P. Taylor, and A. P. M. Moloch [2001a], Electromagnetic wave chaos in gradient refractive index optical cavities, *Phys. Rev. Lett.* 86, 5466{5469.

Wilkinson, P. B., T. M. Fromhold, R. P. Taylor, and A. P. M. Moloch [2001b], Effects of geometrical ray chaos on the electromagnetic eigenmodes of a gradient index optical cavity *Phys. Rev. E* 64, 026203.

Young, L.-S. [1999], Recurrence times and rates of mixing, *Israel J. Math.* 110, 153{188.

Zaslavsky, G. M. [1992], Anomalous transport and fractal kinetics. In *Topological aspects of the dynamics in fluids and plasmas*, eds. H. K. Moffatt et al., pages 481{500, Kluwer, Dordrecht.

Zaslavsky, G. M. [1994a], Fractional kinetic equation for Hamiltonian chaos, *Physica D* 76, 110{122.

Zaslavsky, G. M. [1994b], Renormalization group theory of anomalous transport in systems with Hamiltonian chaos, *Chaos* 4, 25{33.

Zaslavsky, G. M. and S. S. Abdullaev [1997], Chaotic transmission of waves and "cooling" of signals, *Chaos* 7, 182{186.

Zaslavsky, G. M. and M. Edelman [1997], Maxwell's demon as a dynamical model, *Phys. Rev. E* 56, 5310{5320.

Zaslavsky, G. M. and M. Edelman [2000], Hierarchical structures in the phase space and fractal kinetics: I. Classical systems, *Chaos* 10, 135{146.

Zaslavsky, G. M. and M. Edelman [2001], Weak mixing and anomalous kinetics along laminated surfaces, *Chaos* 11, 295{305.

Zaslavsky, G. M., R. Z. Sagdeev, D. A. Ulikov, and A. A. Chencikov [1991], Weak Chaos and Quasi-Regular Patterns. Cambridge Univ. Press, Cambridge.

Zorich, A . [1997], Deviation for interval exchange transformations, Ergodic Theory and Dynamical Systems 17, 1477{1499.

Zwanzig, R . [1983], From classical dynamics to continuous-time random-walks, J. Stat. Phys. 30, 255{262.